

Drag Force and Ventilation Efficiency for Urban-Like Regular Arrays [†]

Mingjie Zhang ^{1,2,*}, Olga Palusci ², Riccardo Buccolieri ^{2,*}, Zhi Gao ¹, and Xin Guo ³

¹ School of Architecture and Urban Planning, Nanjing University; zhgao@nju.edu.cn.

² Dipartimento di Scienze e Tecnologie Biologiche ed Ambientali, Laboratory of Micrometeorology, University of Salento; olga.palusci@unisalento.it

³ Department of Mechanical and Aerospace Engineering, Syracuse University; xguo48@syr.edu

* Correspondence: mzhang@smail.nju.edu.cn (M.Z.); riccardo.buccolieri@unisalento.it (R.B.);

[†] Presented at the 6th International Electronic Conference on Atmospheric Sciences, online, and 15–30 Oct 2023.

Abstract: The present study investigates drag force and ventilation efficiency in urban-like regular arrays, with the aim of uncovering correlations that can enhance the understanding of airflow dynamics in urban environments. The arrangements are sorted into cubic arrays, with uniform size (H^*H^*H) but varying wall-to-wall distances (W), and cuboid arrays, with uniform height H but varying length and W . The planar area density (λ_p) ranges from 0.0625 to 0.56. Three-dimensional computational fluid dynamics (CFD) simulations employing the standard k- ϵ turbulence model are performed following the grid sensitivity test and validation against wind tunnel data. The bulk drag force (F), frontal area averaged drag force ($F_{A,ave}$), normalized spatially averaged velocity (U_{ave}/U_H), and air change rate (ACH) are calculated. It is found that F shows a marked increase for $0.0625 < \lambda_p < 0.25$ and a gradual increase for $0.25 < \lambda_p < 0.56$. Further linear regression analysis shows that U_{ave}/U_H and ACH are strongly negatively correlated with F , which supports the effectiveness of drag force in reflecting ventilation efficiency, particularly for evaluating urban block-scale ventilation.

Keywords: Scale-model arrays; Planar area density; Drag force; CFD; Air change rate; Regression analysis

1. Introduction

Urban ventilation plays a crucial role in maintaining air quality and mitigating the heat island effect in urban areas [1]. It facilitates the movement of fresh air, disperses pollutants, and regulates temperature, creating a healthier and more comfortable environment for residents. Researchers conducted experimental and numerical studies on how urban ventilation efficiency was influenced by urban geometries. One important aspect is to explore the buildings' resistance to urban airflow, which can be represented by the drag force (F) or drag coefficient. Previous studies measured F for different urban-like geometries in a wind tunnel [2, 3]; results showed that F first significantly increases and then slightly decreases with the planar area density (λ_p , i.e., the ratio of the building footprint to the lot area), and the force mostly acts on the first-row buildings. Two questions remain for further exploration, including "Could the simulated F be validated against measured values?" and "Could the F indicate the local ventilation efficiency?". The aim of the present study is to explore these by numerically investigating urban-like block arrays.

The paper is structured as follows: the investigated subcases are described in Section 2; CFD settings, grid sensitivity test, and model validation method are introduced in Section 3; comparison of simulated and measured F , discussion on the impact of λ_p on F and $F_{A,ave}$, and on the correlation between F and U_{ave}/U_H , ACH are presented in Section 4 followed by the summary of main conclusions in Section 5.

Citation: To be added by editorial staff during production.

Academic Editor: Firstname Last-name

Published: date



Copyright: © 2023 by the authors. Submitted for possible open access publication under the terms and conditions of the Creative Commons Attribution (CC BY) license (<https://creativecommons.org/licenses/by/4.0/>).

2. Description of the Investigated Cases

Figure 1 shows the investigated two groups of regular-layout block arrays. The arrays differ for the planar shape of buildings. Case Cr represents cube-shaped regular-layout arrays, while Case Cr* represents cuboid-shaped regular-layout arrays. All buildings have a uniform height (H) of 0.02 m. The distance between buildings (W) varies. Specifically, W for Cases Cr ranges from $3H$ to $0.33H$; W for Cases Cr* ranges from $1.5H$ to $0.5H$. In the two groups, λ_p presents different values, i.e., 0.0625, 0.11, 0.25, 0.44, and 0.56. The height-to-width ratio (H/W) varies from 0.33 to 3. The number of buildings (n) for Cases Cr varies from 16 to 100, and n for Cases Cr* equals 49. The details for Case Cr and Cr* are summarised in Table 1, e.g., Case Cr-1 consists of 16 cubes with W of $3H$, with H/W of 0.33, with λ_p and frontal area ratio (λ_f) of 0.0625. Case Cr*-1 consists of 49 cuboids with W of $1.5H$, H/W of 0.67, λ_p of 0.0625, and λ_f of 0.125.

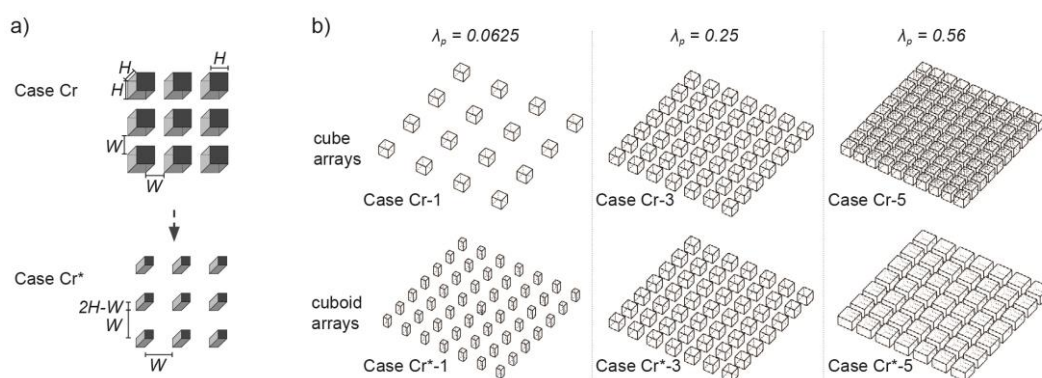


Figure 1. Two groups of block arrays investigated in this work; (a) diagram of the form types; H : building height; W : distance between buildings; (b) sketches of example subcases; λ_p : planar area density.

Table 1. Details for investigated subcases.

Group	Subcases	Layout / Building form	Lot area	n	W	H/W	λ_p	λ_f
Case Cr	1			4×4	3H	0.33	0.0625	0.0625
	2	Regular /		5×5	2H	0.5	0.11	0.11
	3 ^a	Cube with size of	13H×13H	7×7	H	1	0.25	0.25
	4	H^*H^*H		9×9	0.5H	2	0.44	0.44
	5			10×10	0.33H	3	0.56	0.56
Case Cr*	1		12.5H×12.5H		1.5H	0.67	0.0625	0.125
	2	Regular / Cuboid with	12.67H×12.67H		1.33H	0.75	0.11	0.167
	3 ^a	side width 2H-W,	13H×13H	7×7	H	1	0.25	0.25
	4	constant height H	13.33H×13.33H		0.67H	1.5	0.44	0.33
	5		13.5H×13.5H		0.5H	2	0.56	0.375

^a Case Cr-3 is the same to Case Cr*-3;

3. Numerical Calculation of Drag Force

3.1. CFD Settings and Grid Sensitivity Test

Figure 2 shows the computational domain setting for Case Cr-3, taken as an example. Considering the symmetry of the array, only half domain was modeled to save computational cost. The domain size was set following the AIJ guidelines [5]. The height of the domain is $11H$, while the upstream, downwind, and lateral domain lengths are $5H$, $15H$, and $7H$, respectively. The blockage ratio of 2.4% fulfilled the requirement of the guideline. The CFD code ANSYS FLUENT 16.0 was used to solve the steady-state Reynolds-averaged Navier Stokes (RANS) equations closed by the standard $k-\epsilon$ turbulence model. The

standard wall functions based on the work of Launder and Spalding [4] were employed, and smooth wall conditions (sand-grain roughness height k_s : 0; roughness constant C_s : 0.5) were imposed at building surfaces and ground (representing the wind tunnel floor downstream of the roughness elements, including the turntable). The second-order discretization scheme was used for the pressure, and the second-order upwind discretization schemes were used for the momentum, k , and ϵ . The SIMPLE scheme was used for the pressure–velocity coupling. The default under-relaxation factors were used, such as 0.3 for pressure, 0.7 for momentum, 0.8 for k , and ϵ . The converge criteria was that the scaled residuals reached 10^{-5} for continuity and 10^{-6} for other field variables.

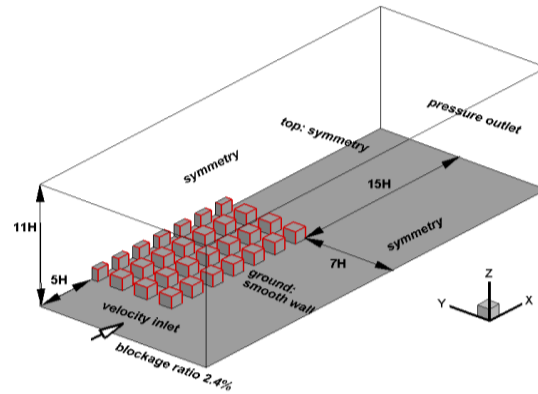


Figure 2. Computational domain setting following the AIJ guidelines.

By fitting the data from the wind tunnel test, the inflow profiles for the velocity (U_z) and turbulent intensity (I_z) were obtained as follows:

$$\frac{U_z}{U_H} = 1.024 \left(\frac{Z}{H}\right)^{0.16} \quad (1)$$

$$\frac{I_z}{I_H} = \left(\frac{Z}{H}\right)^{-0.07} \quad (2)$$

where Z is the height, H is the building height of 0.02 m, U_H and I_H is the velocity and turbulent intensity at roof level, which are 4.3 m/s and 27.8% respectively.

A grid sensitivity test for Case Cr-3 was performed by considering three grids with linear scale factor $\sqrt{2}$. All three grids employed hexahedral cells. The total cell numbers for coarse, basic, and fine grids were 1,164,013, 2,497,754, and 5,512,388, respectively. To assess the grid sensitivity, the grid convergence index (GCI) [6] was employed and evaluated for non-dimensional values of averaged streamwise velocity ($U_{ave,x}/U_H$) and averaged turbulent kinetic energy (TKE_{ave}/TKE_H) over vertical and horizontal middle lines of the six canyons of the middle column (Figure 3a). Note that TKE_H is the turbulent kinetic energy of the incoming flow at the roof level. The GCI values for the investigated lines for the basic grid were $\leq 5\%$, except that of the TKE_{ave}/TKE_H for the vertical middle line of the first canyon, which was about 6%. The test supported that the basic grid could achieve grid-independent results.

3.2. Drag Force and Ventilation Indices

The bulk drag force (F [N]), the frontal area averaged drag force ($F_{Af,ave}$ [N/ m²]), the normalized spatially averaged velocity (U_{ave}/U_H), and the air change rate (ACH [s⁻¹]) are investigated. The $F_{Af,ave}$ is obtained by dividing F by the frontal area (A_f [m²]) for each sub-case. The U_{ave} is obtained by calculating the volume-averaged velocity magnitude for the whole block canopy layer. As for the ACH , it was calculated by dividing the total inflow/outflow rate (q [m³/s]), obtained by determining the bulk flow balance, by the volume of block canopy (V [m³]).

3.3. Experimental Validation

The numerical simulations performed in this study were compared against wind tunnel measurements performed in a previous study [2] conducted at the Faculty of Engineering and Sustainable Development of the University of Gavle (Sweden). The employed closed-circuit equilibrium boundary layer (BL) flow wind tunnel had a working section of 11 m long, 3 m wide, and 1.5 m high. The BL flow was achieved considering cubes of 0.04 m representing roughness elements. The distance between the final row of roughness elements and the front of the lot area was approximately 0.4 m (20 times the array height H). The standard load cell method was used to measure F acting on the cube arrays. The validation was done by comparing the drag force generated by the cube-regular block arrays Cases Cr with λ_p from 0.0625 to 0.56, under the inflow condition with reference inflow velocity (U_H) of 4.3 m/s.

4. Results and Discussion

4.1. Comparison of the Measured and Simulated Drag Force

The simulated F for the five subcases among Cases Cr with different λ_p were compared with the wind-tunnel measured values (Table 2).

Table 2. Comparison of the simulated and measured drag force (F) for Cases Cr.

Subcases	λ_p	F (N)		Difference
		Experiment	CFD	
Case Cr	1	0.073	0.062	-14.7%
	2	0.090	0.076	-14.9%
	3	0.105	0.092	-12.8%
	4	0.098	0.100	2.3%
	5	0.091	0.102	11.9%

It is found that the simulations are generally consistent with the wind tunnel experiment. Absolute values of relative errors are up to 14.9%. Specifically, for Cases Cr-1, Cr-2, and Cr-3 with lower λ_p , the simulation slightly underestimated the F ; while for Cases Cr-4 and Cr-5 with higher λ_p , the simulation would slightly overestimate the F . The measured F ranges from 0.073 N to 0.105 N; while the simulated F ranges from 0.062 N to 0.102 N. Numerical results did not reproduce the variation trend of F shown in the experiments, i.e., F first increases for $0.0625 < \lambda_p < 0.25$ and then slightly decreases for $0.25 < \lambda_p < 0.56$. This point needs more investigation in future work, e.g., testing the divergence of drag force for different rows of cubes in Case Cr-3.

4.2. Impact of Urban Form on Drag Force

Figure 3a analyzes the relations between bulk drag force F and λ_p , taking three subcases for Cases Cr and Cr* as examples. For Cases Cr of cubic arrays, F shows a marked increase (47.6%) for $0.0625 < \lambda_p < 0.25$ and a gradual increase (11.2%) for $0.25 < \lambda_p < 0.56$; for Cases Cr* of cuboid arrays, a similar trend is found though the difference for the increase rate of F in these two intervals is less significant, respectively 28.3% and 16.7%. As also displayed in Figure 3a, Cases Cr have an increase of H/W , i.e., from 0.33 to 1, then to 3; while Cases Cr* have an increase of H/W , i.e., from 0.67 to 1, then to 2. It can be concluded that F shows a marked increase for $0.33 < H/W < 1$ and a gradual increase for $1 < H/W < 3$. The relations between frontal area averaged drag force $F_{Af,ave}$ and λ_p are analyzed in Figure 3b. $F_{Af,ave}$ shows a marked decrease for $0.0625 < \lambda_p < 0.25$ and a gradual decrease for $0.25 < \lambda_p < 0.56$ for both Cases Cr and Cr*. Considering all subcases, L_f displays a more direct relation with $F_{Af,ave}$, i.e., a larger increase in λ_f results in a larger decrease of $F_{Af,ave}$, than that between H/W with F , i.e., a larger increase in H/W doesn't guarantee a larger decrease of F .

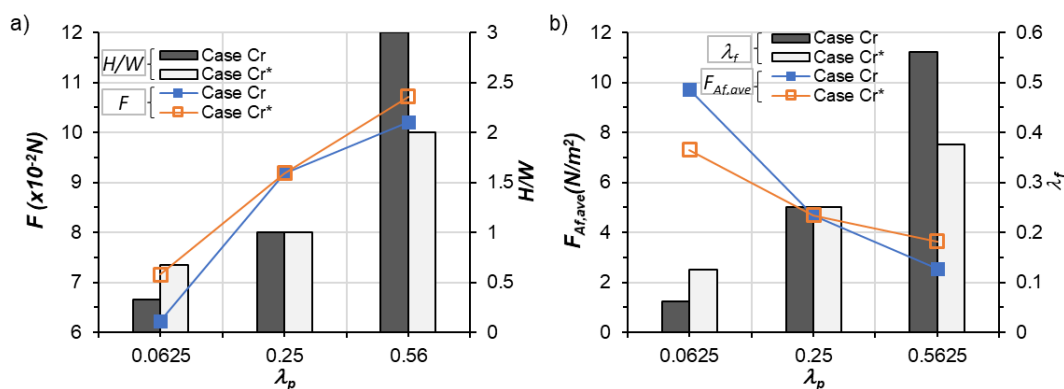


Figure 3. Analysis of the impact of urban form on drag force: a) relation between bulk F and λ_p ; b) relations between frontal area averaged drag force $F_{Af,ave}$ and λ_p .

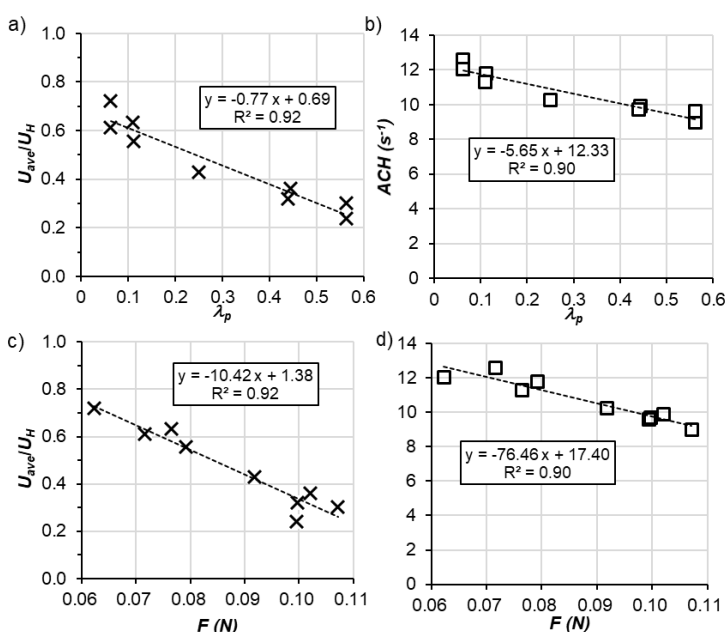


Figure 4. Analysis for all the subcases of Case Cr and Cr*: (a-b) linear regression analysis between λ_p and U_{ave}/U_H and ACH ; (c-d) linear regression analysis between F and U_{ave}/U_H and ACH .

4.3. Correlation between Drag Force and Ventilation Indices

Considering the investigated cube and cuboid arrays, strong negative correlations between λ_p and the U_{ave}/U_H and ACH are found by linear regression analysis, as shown in Figures 4a and 4b. This is consistent with previous studies but need further explored particularly on block arrays with other different types of forms. As Figures 4c and 4d show the U_{ave}/U_H and ACH are negatively correlated with F . This supports that F serves as a ventilation efficiency index: a higher F means a lower ventilation efficiency, and vice versa.

5. Conclusions

This work investigated cube-regular and cuboid-regular arrays with different values of the planar area density (λ_p) to investigate the relation between urban ventilation and drag force. The steady-state simulations are performed using the standard $k-\varepsilon$ turbulence model to calculate the bulk drag force (F), the frontal area averaged drag force ($F_{Af,ave}$), the normalized spatially averaged velocity (U_{ave}/U_H), and the air change rate (ACH , s^{-1}). The computational settings follow the best guidelines and a grid sensitivity test is conducted. A comparison of the simulated F for cube-regular arrays with the values measured in a previous wind tunnel test shows a good agreement (relative error $\pm 15\%$). Through the analysis of the investigated cases, it is found: i) F shows a marked increase for $0.0625 < \lambda_p < 0.25$ and a slight increase for $0.25 < \lambda_p < 0.56$; ii) the varying trend is more significant for cube arrays than cuboid arrays; however, it should be noted that the simulation results didn't report a similar slight decreasing trend of F for $0.25 < \lambda_p < 0.56$ reported in a previous experiment; iii) for both cube arrays and cuboid arrays, $F_{Af,ave}$ decrease with the increase of λ_p , and larger increase of λ_f guarantees a larger decrease of $F_{Af,ave}$; iv) the spatially averaged velocity (U_{ave}) and air change rate (ACH) are strongly negatively correlated with F . The ability of F in reflecting ventilation efficiency proves that it can serve as an index, particularly for evaluating urban block-scale ventilation.

Author Contributions: Conceptualization, formal analysis, validation, writing—original draft preparation, writing—review and editing, M.Z.; conceptualization, validation, writing—review and editing, supervision, O.P. and R.B.; writing—review and editing, project administration, Z.G.; software, visualization, X.G.. All authors have read and agreed to the published version of the manuscript.

Funding: The work was financially supported by the Postgraduate Research & Practice Innovation Program of Jiangsu Province (No. KYCX22_0161) and the National Natural Science Foundation of China (Grant No. 52278110).

Acknowledgment: Mingjie Zhang acknowledges China Scholarship Council for Grant No. 202206190148. Olga Palusci acknowledges the Apulia Region for supporting her research work within the framework of the regional program RIPARTI at the University of Salento (Grant No. 32251bed). Riccardo Buccolieri acknowledges the financial support from ICSC–National Research Center in High Performance Computing, Big Data and Quantum Computing, funded by European Union–Next Generation EU - Project name: PNRR-HPC; Project No. CN0000013; CUP: F83C22000740001.

Conflicts of Interest: The authors declare no conflict of interest. The funders had no role in the design of the study; in the collection, analyses, or interpretation of data; in the writing of the manuscript; or in the decision to publish the results.

References

1. Buccolieri, R.; Sandberg, M.; Di Sabatino, S. City breathability and its link to pollutant concentration distribution within urban-like geometries. *Atmos. Environ.* **2010**, *44*(15), 1894–1903.
2. Buccolieri, R.; Wigö, H.; Sandberg, M.; Di Sabatino, S. Direct measurements of the drag force over aligned arrays of cubes exposed to boundary-layer flows. *Environ. Fluid Mech.* **2017**, *17*(2), 373–394.
3. Buccolieri, R.; Sandberg, M.; Wigö, H.; Di Sabatino, S. The drag force distribution within regular arrays of cubes and its relation to cross ventilation – Theoretical and experimental analyses. *J. Wind Eng. Ind. Aerodyn.* **2019**, *189*, 91–103.
4. Launder, B.E.; Spalding, D.B. The numerical computation of turbulent flows. *Comput. Meth. Appl. Mech. Eng.* **1974**, *3*(2), 269–289.
5. Tominaga, Y.; Mochida, A.; Yoshie, R.; Kataoka, H.; Nozu, T.; Yoshikawa, M.; Shirasawa, T. AIJ guidelines for practical applications of CFD to pedestrian wind environment around buildings. *J. Wind Eng. Ind. Aerodyn.* **2008**, *96*(10–11), 1749–1761.
6. Roache, P.J. Quantification of uncertainty in computational fluid dynamics. *Annu. Rev. Fluid Mech.* **1997**, *29*(1), 123–160.

Disclaimer/Publisher's Note: The statements, opinions and data contained in all publications are solely those of the individual author(s) and contributor(s) and not of MDPI and/or the editor(s). MDPI and/or the editor(s) disclaim responsibility for any injury to people or property resulting from any ideas, methods, instructions or products referred to in the content.